

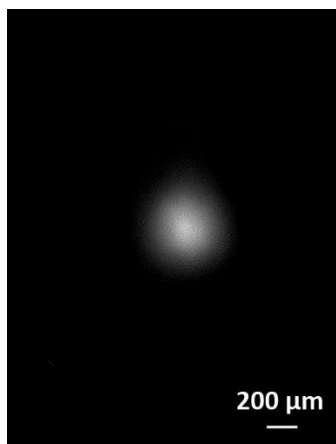
Electronic Supporting Information for

Spatially resolved microfluidic stimulation of lymphoid tissue ex vivo

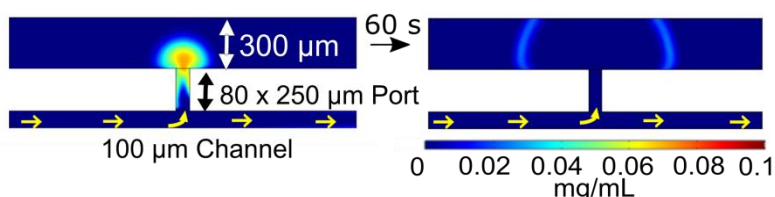
Ashley E. Ross¹, Maura C. Belanger¹, Jacob F. Woodroof¹, Rebecca R. Pompano^{1,2}

University of Virginia

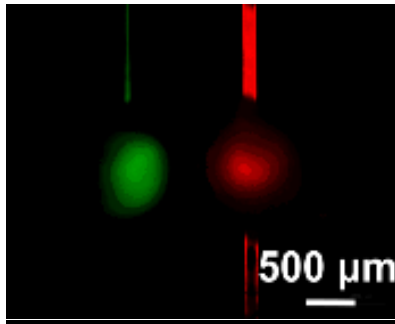
Supporting Movies:



SI Movie 1: Delivery and flushing of FITC-Dextran to a lymph node slice. A pulse of FITC-labelled 40-kDa-Dextran (0.1 mg/mL; white) was delivered for 5 s to a tissue slice at a flow rate of 0.4 $\mu\text{L}/\text{min}$. After delivery, dextran was removed from the slice by continued flow of PBS at a rate of 0.2 $\mu\text{L}/\text{min}$. Movie plays at 2x speed. Scale bar is 200- μm .



S1 Movie 2: Simulated delivery and flushing of FITC-Dextran to a porous matrix. A simulated 5-s pulse of FITC-labelled 40-kDa-Dextran (0.1 mg/mL), followed by flushing with saline through the porous matrix. Movie plays at 10x speed.



SI Movie 3: Dual stimulation of lymph node slices. Two pulses were delivered to the same tissue slice through different ports. FITC-labelled 70-kDa-Dextran (0.1 mg/mL; green) was delivered for 5 s through one channel, and Texas Red-labelled 10-kDa-Dextran (0.1 mg/mL; red) was delivered for 8 s through a different channel. Flow rates were 0.4 $\mu\text{L}/\text{min}$ for each. The two deliveries were staggered in time, and each was immediately followed by flow of PBS. After completion of the 10-kDa dextran delivery, the flow rate for PBS was ramped in both channels to 5 $\mu\text{L}/\text{min}$ to completely clear the tissue. Movie plays in real time. Scale bar is 500- μm .

Supplemental Methods:

COMSOL Multiphysics Model:

A computational model was used to predict the delivery profile of dextran in the tissue as a function of initial concentration and flow rate through the microfluidic channel. The two-dimensional model was built in COMSOL Multiphysics 5.2 and incorporated equations of incompressible Navier-Stokes flow through the channel and port as well as isotropic diffusion and convection into the tissue (COMSOL modules: Free and porous media flow; Transport of diluted species in porous media). Fluid flowed into a 100- μm channel and out through the port and a waste outlet set to atmospheric pressure. The dextran solution was modelled with the density and viscosity of water, 1000 kg/m^3 and 1.00 $\text{mPa}\cdot\text{s}$. The inflow velocity was set to 6.67×10^{-4} m/s (flow rate 0.4 $\mu\text{L}/\text{min}$ through a 100 μm x 100 μm channel) unless otherwise noted.

The tissue was modeled as a porous matrix (300 μm thick) and set as an open boundary to allow diffusion out the top and sides of the tissue (except for in Figure 3, tissue was set as a closed boundary on top for comparison). The diffusion coefficient through the tissue, D [m^2/s], was initially defined in the program as

$$D = \frac{\epsilon_p}{\tau} D_{free} \quad (1),$$

where D_{free} is the diffusion coefficient in free solution [m^2/s], ϵ_p is the (unitless) porosity of the tissue, and τ is the (unitless) tortuosity, a measure of the hindrance of diffusion through the tissue. Porosity and tortuosity were set to 0.2 and 2.0, respectively, based on experimental estimates in brain tissue ¹. Definitions for τ vary, and the value used was based on the definition ²

$$\tau = \sqrt{\frac{D_{free}}{D_{coef}}} \quad (2).$$

To account for this difference in definition, we manually squared the value for tortuosity in the program, to obtain a corrected equation for D :

$$D = \frac{\epsilon_p}{\tau^2} D_{free} \quad (3).$$

The diffusion coefficient for 40-kDa dextran used in the model was $4.2 \times 10^{-11} m^2/s$ ³.

The initial concentration of dextran was set to zero throughout the channel, port, and tissue. To model a 5-s pulse of dextran, the concentration at the inlet of the simulated channel was set to a step function that started at $2.5 \times 10^{-3} mol/m^3$ and dropped to $0 mol/m^3$ after 5 s unless otherwise noted.

Preliminary tests indicated that the model was highly sensitive to the permeability of the porous matrix. Permeability was set empirically to approximate the experimental results for a 5-s delivery of 40-kDa dextran, specifically the time needed to reach maximum concentration directly above the port (5 s; measured half-way through the simulated tissue) and the pulse width (Figure S6). The value obtained was $3 \times 10^{-12} m^2$, which is similar to the value obtained for simulating interstitial flow through lymph node ⁴.

The model was solved using a triangular mesh. The steady state flow profile was calculated and used to solve the time-dependent mass transport problem. To test the effect of flow parameters on distribution of dextran through the tissue, the delivery time (3 – 60 s), inflow velocity (0.2 - 0.6 $\mu\text{L}/\text{min}$), and initial concentration at the inlet (0.1 – 0.2 mg/mL) were varied. Dextran concentration was reported along a bisecting line through the simulated tissue (half-way deep). The profile at the time of maximal intensity over the port was exported and fit with a Gaussian curve in Graphpad Prism in the same manner as experimental linescan data, to obtain the area under the curve and the pulse width.

Supporting Figures:

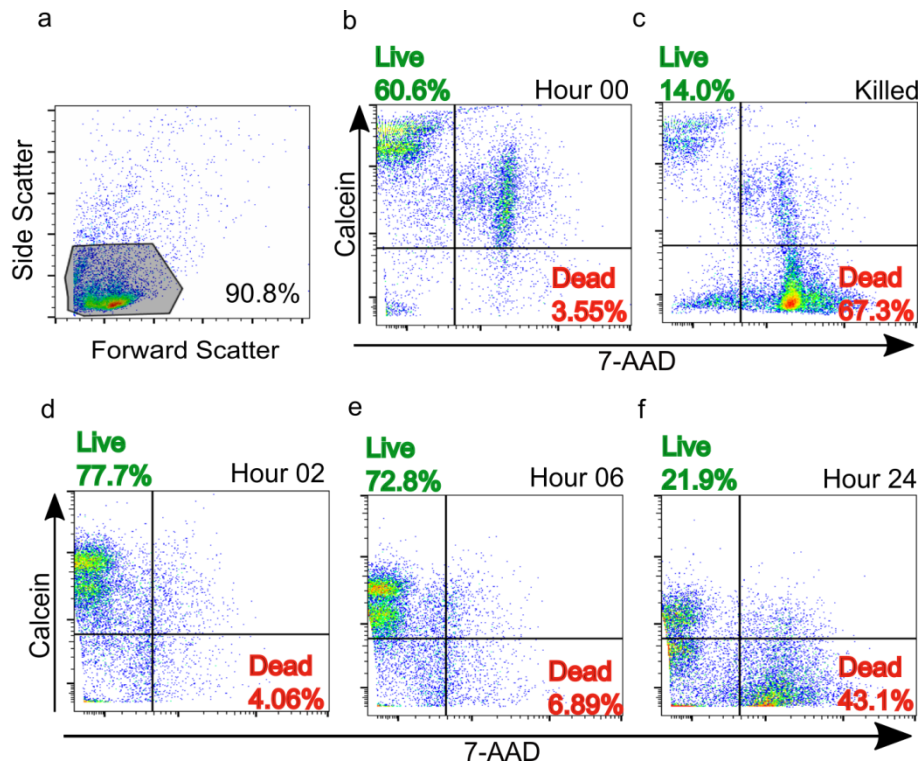


Figure S1: Cells in murine lymph node slices are viable for at least 6 hr. Twenty slices for each condition (N=5 mice) were collected, incubated 1 hr at 37 °C with 5 % CO₂ to recover, then further incubated for 0, 2, 6, and 24 hours before being crushed, pooled, and stained with calcein AM (stains live cells) and 7-AAD (stains dead cells). Cells were analyzed by flow cytometry. Lymphocytes were (a) gated on scatter and (b-f) analyzed for calcein and 7-AAD intensity. Slices treated with ethanol (c) were used to set quadrants. The large double positive region at hr 0 (b) resolves into live cells by hr 2 (d), indicating that it may be attributable to damaged cell membranes and that the 1 hr recovery period should be lengthened. Slices increased in viability from 0 to 2 hour (60 % and 78 % viable, respectively, indicating that a recovery period is necessary, much like in brain slice culture.⁵ Viability decreased between 6 and 24 hours, from 73 % to 22 %. These experiments show that lymph node slices are viable in immersion culture for at least 6 hours after slicing.

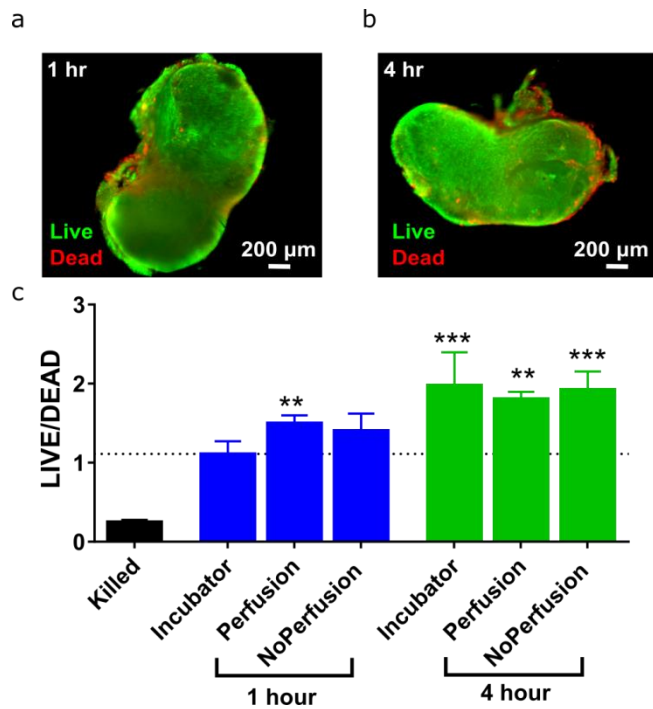


Figure S2: Testing the viability of lymph node slices on-chip. Lymph node slices were collected and allowed to recover for 1 hr while immersed in media in a cell culture incubator at 37 °C with 5% CO₂. Next, slices were cultured for 1 hr or 4 hr on chip, with and without perfusion over the tissue slice. Slices left in the cell culture incubator were used as positive controls, and slices treated with 70% ethanol for 10 minutes were used as negative (killed) controls. After each time point, slices were stained with a LIVE/DEAD assay (Calcein AM/propidium iodide). (a, b) Representative images from on-chip culture without perfusion after 1 and 4 hr. (c) Quantitative analysis of fluorescence using a ClarioSTAR plate reader to determine the ratio of Calcein to PI staining. A line is drawn at the average ratio of the 1 hour positive control (1.11) as a point of reference. The ratio of LIVE/DEAD was significantly dependent on treatment type (one-way ANOVA, $p < 0.001$, $n = 4$). Asterisks indicate conditions that were significantly different from the killed control (Bonferroni post-tests, ** $p < 0.005$, *** $p < 0.001$). An increase in viability was seen between 1 and 4 hrs, indicating that an extended resting period may be needed after dissection and slicing.

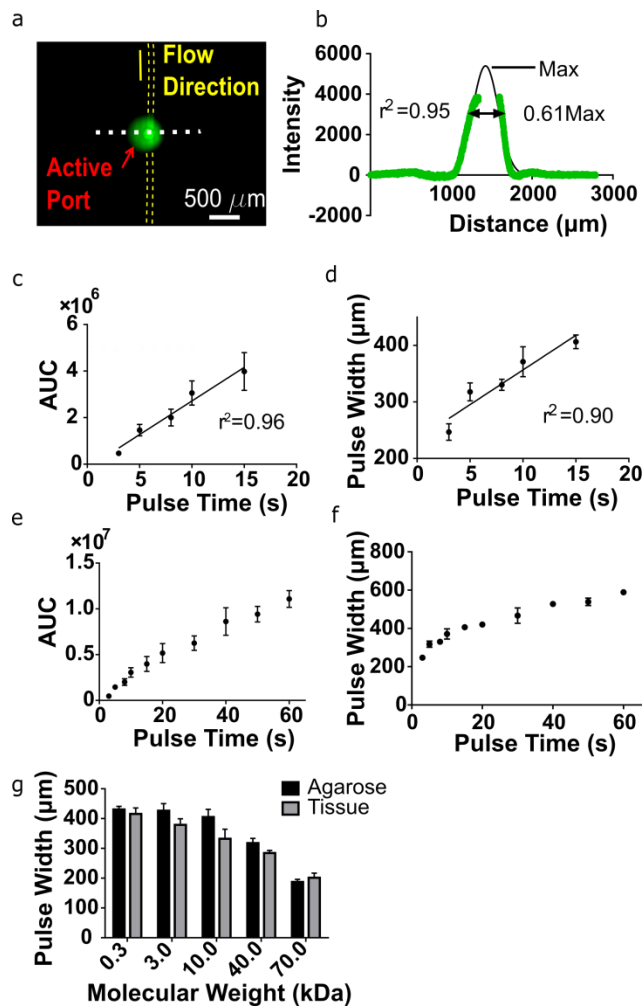


Figure S3: Delivery of 40-kDa FITC-Dextran to 300 μm-thick 2% slices of agarose. a) Fluorescent image of 40-kDa FITC-Dextran delivery to an agarose pad (Scale bar is 500 μm). Channel is highlighted in the yellow dotted line to show direction of flow. The dye (green) exits through the active port and diffuses through the agarose pad. White dotted line shows line scan. b) Fluorescent intensity vs. distance along the linescan after a 5-s delivery. More concentrated dextran is inside the port and easily visible through the agarose pad, which causes a false increase in fluorescent intensity across the port. To circumvent this artefact, a portion of the data was excluded at the port. The curve was assumed to be Gaussian because the more complex sample (tissue) also followed a Gaussian distribution. Data was fit with a Gaussian distribution curve and had a correlation of fit of 0.95. Width of the peak was taken at 61% of the max (2 standard deviations). c) Area under curve increased linearly with increasing delivery time (pulse time) but does not remain linear at longer pulse times (e). d) Pulse width increased linearly at low pulse times (e, $r^2=0.9014$) and began to plateau at longer pulse times (f). g) On average, pulse width significantly decreased with increasing molecular weight for both 2 % agarose and tissue (tissue data same as in Figure 2 for 5-s pulse). (n =4-5, mean ± SEM)

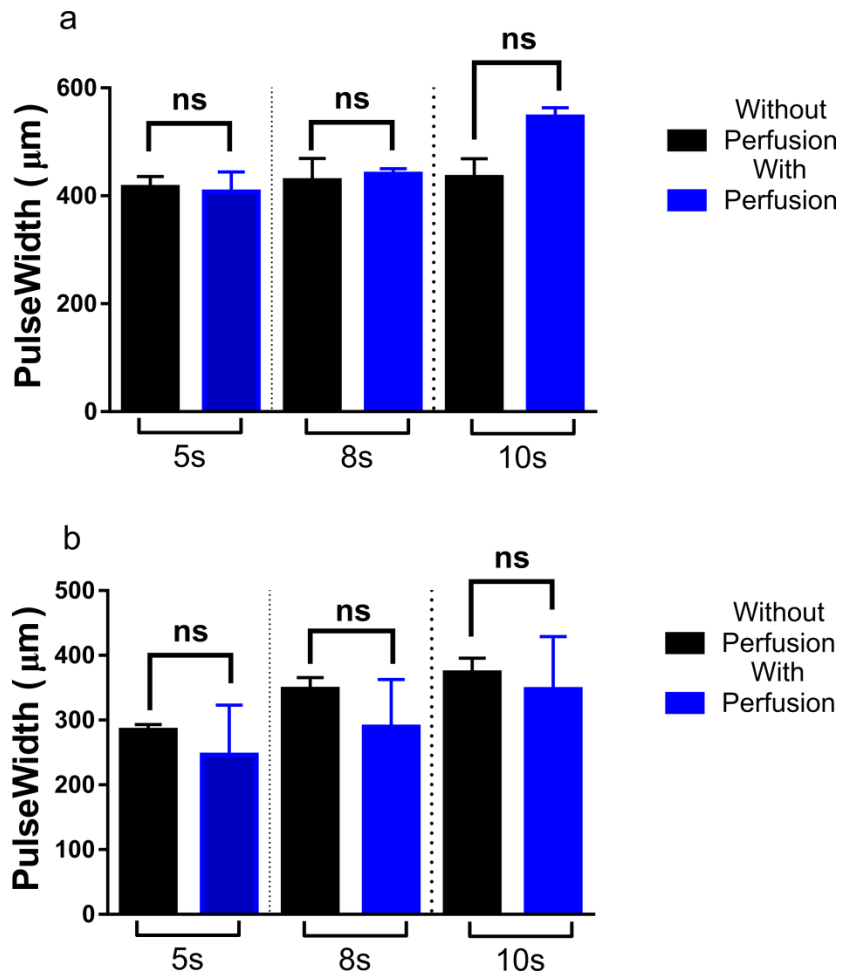


Figure S4: Perfusion did not significantly affect the distance spread in tissue. a) Pulse width was compared with (blue) and without (black) 0.5 mL/min perfusion of 1x PBS over tissue slices after 5-s, 8-s, and 10-s delivery times of (A) 0.1 mg/mL fluorescein and (b) 0.1 mg/mL 40 kDa FITC-Dextran. The spread at each time point was not significantly different with or without perfusion ((one-way ANOVA, Bonferroni post-tests, $p > 0.05$).

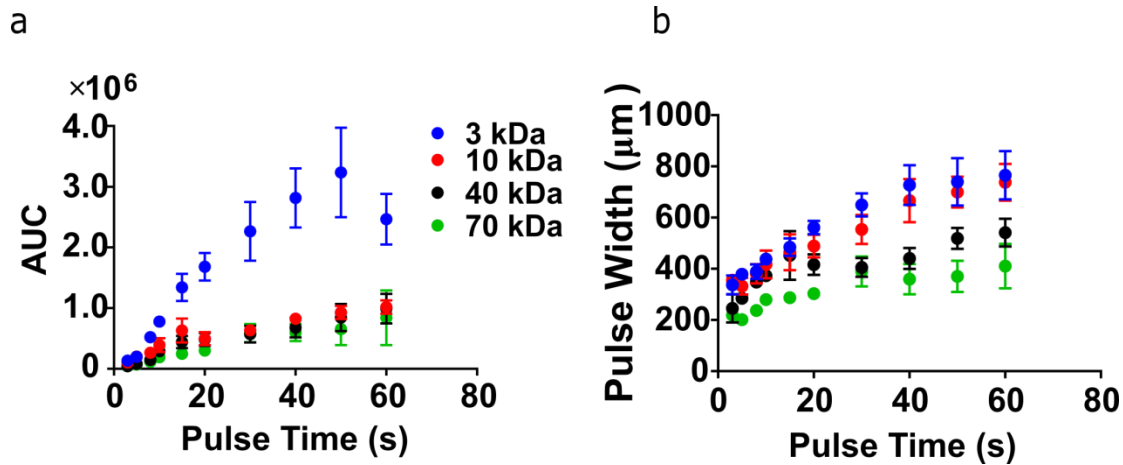


Figure S5: Quantity and spread of dextran in tissue with increasing pulse times. (a) Area under the curve, AUC, and (b) pulse width began to plateau for delivery times greater than 15 seconds, for all dextrans. The AUC values for 3 kDa were larger than the values for the rest of the dextrans because the dye was brighter, which raised the intensity of the peak. Data for 40-kDa dextran is repeated from Figure 3 in the main text.

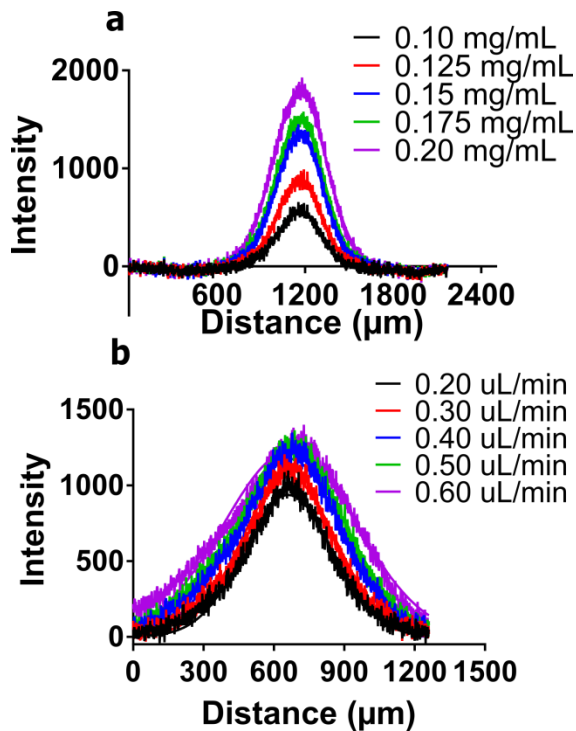


Figure S6: Line scan data for delivery of 40-kDa FITC-dextran for varying concentrations and total flow rates to lymph node tissue. Background fluorescence was subtracted out by subtracting the baseline fluorescent signal before delivery. a) Area under the curve increased with increasing delivery concentration of 40 kDa FITC-Dextran, while pulse width remained relatively constant. b) Area under the curve and pulse width both increased with increasing delivery flow rate

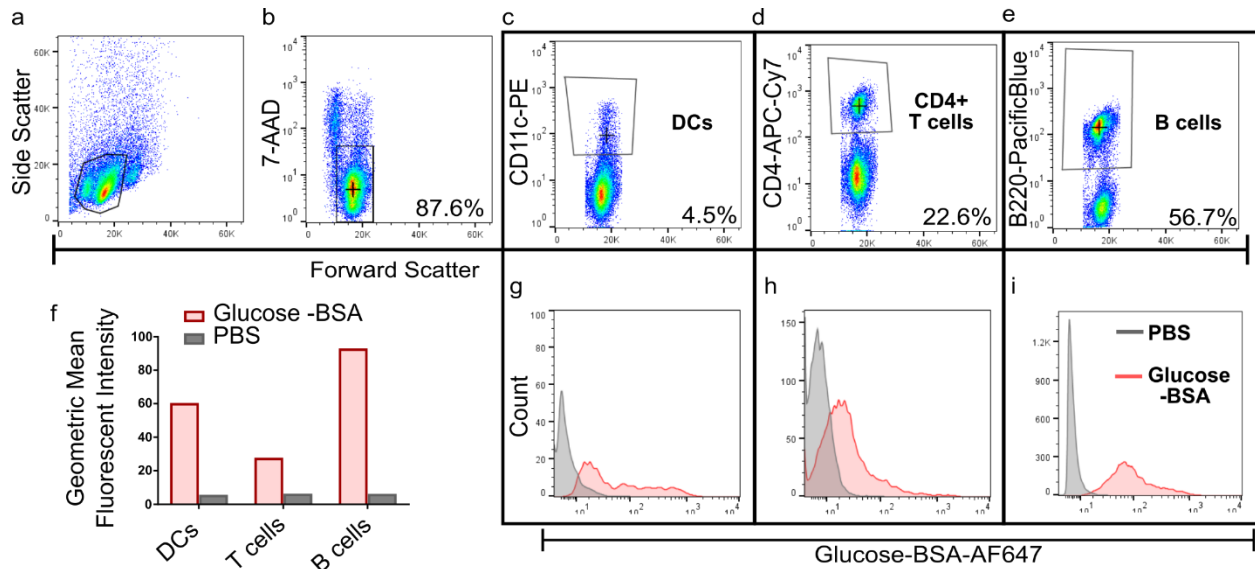


Figure S7: Glucose-BSA is taken up by B-cells, T-cells, and dendritic cells. Pooled splenocytes were incubated with 400 $\mu\text{g}/\text{mL}$ AlexaFluor 647-labelled glucose-BSA or PBS in vitro for 1 hr, washed, and analyzed by flow cytometry. Cells were immunostained with B220-Pacific blue, CD4-APC-Cy7, and CD11c-PE. Gating strategy: (a) forward and side scatter to identify lymphocytes, (b) live cells (7-AAD negative), (c, d, e) CD11c+ DCs, CD4+ T cells, and B220+ B cells gated based on FMO controls (not shown). (f, g-i) Each population was analyzed for glucose-BSA uptake. All cell types picked up the glucose-BSA; geometric mean fluorescent intensity was greatest for the B-cells, followed by the DCs and T-cells.

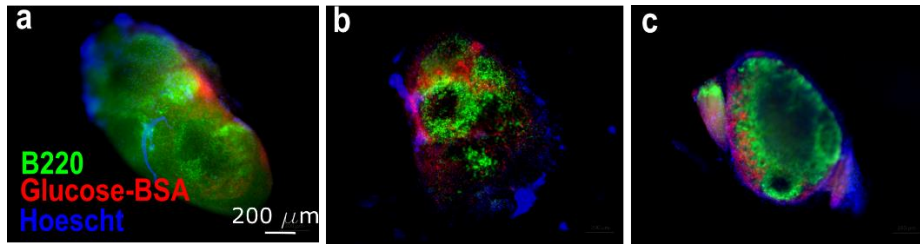


Figure S8: Soaking lymph node tissue slices with Alexa Fluor 657-Glucose-BSA resulted in varying levels and locations of glucose uptake. Live lymph node slices were stained with 10 $\mu\text{g}/\text{mL}$ FITC anti-mouse CD45R/B220 antibody (clone RA3-6B2) and 1 $\mu\text{g}/\text{mL}$ Hoescht 33342 trihydrochloride trihydride. Each slice in a-c was soaked with 400 $\mu\text{g}/\text{mL}$ of Alexa Fluor 657-Glucose-BSA for 1 hour, and all slices were collected from the same mouse. This variation argues for the need for local activation if a particular region is of interest, without relying on the biological variation amongst lymph node slices and/or mice.

Supporting References:

- 1 E. Syková and C. Nicholson, Diffusion in Brain Extracellular Space. *Physiol. Rev.*, 2008, **88**, 1277–1340.
- 2 J. Hrabec, S. Hrabětová and K. Segeth, A Model of Effective Diffusion and Tortuosity in the Extracellular Space of the Brain. *Biophys. J.*, 2004, **87**, 1606–1617.
- 3 C. Nicholson and L. Tao, Hindered diffusion of high molecular weight compounds in brain extracellular microenvironment measured with integrative optical imaging. *Biophys. J.*, 1993, **65**, 2277–2290.
- 4 L. J. Cooper, J. P. Heppell, G. F. Clough, B. Ganapathisubramani and T. Roose, An Image-Based Model of Fluid Flow Through Lymph Nodes. *Bull. Math. Biol.*, 2015, **78**, 52–71.
- 5 L. Ankri, Y. Yarom and M. Y. Uusisaari, Slice It Hot: Acute Adult Brain Slicing in Physiological Temperature. *JoVE J. Vis. Exp.*, 2014, e52068.